SCIENCE CHINA
Earth Sciences

•RESEARCH PAPER•

May 2021 Vol.64 No.5: 813–824
https://doi.org/10.1007/s11430-020-9730-2

Dust storms in northern China during the last 500 years

Shuang ZHANG[1], Hai XU[1*], Jianghu LAN[2], Yonaton GOLDSMITH[3], Adi TORFSTEIN[3], Guilin ZHANG[1], Jin ZHANG[1], Yunping SONG[1], Kang'en ZHOU[2], Liangcheng TAN[2], Sheng XU[1], Xiaomei XU[4] & Yehouda ENZEL[3]

[1] *Institute of Surface-Earth System Science, School of Earth System Science, Tianjin University, Tianjin 300072, China;*
[2] *State Key Laboratory of Loess and Quaternary Geology, Institute of Earth Environment, Chinese Academy of Sciences, Xi'an 710061, China;*
[3] *Institute of Earth Sciences, the Hebrew University of Jerusalem, Jerusalem 91904, Israel;*
[4] *Department of Earth System Science, University of California, Irvine, CA 92697, USA*

Received August 5, 2020; revised January 10, 2021; accepted January 25, 2021; published online March 22, 2021

Abstract The history and mechanisms of dust storms in northern China remain unclear owing to the paucity of reliable long-term, high-resolution geological records. In this study, we reconstructed the dust storm history of the last ~500 years in northern China, based on sedimentary coarse fraction (>63 μm) of a well-dated core from Lake Daihai, Inner Mongolia. The high-resolution data reveal three intervals of frequent dust storms: AD 1520–1580, AD 1610–1720, and AD 1870–2000. The dust storm events in the Lake Daihai area were broadly synchronous with those inferred from other historical or geological records and generally occurred during cold intervals. Changes in the intensity of Siberian High and the westerlies modulated by temperature variations are the likely major factors controlling dust storm dynamics. An interesting feature is that although the intensities of dust storms have been systematically increased during the recent warming period, a clear decreasing trend within this period is evident. The recent increase in average dust storm intensity may be ascribed to an increase in particle supply resulting from a rapid increase in human activity, whereas the weakening trend was likely caused by decreases in average wind speed resulting from the recent global warming.

Keywords Dust storm, Lake Daihai, Temperature, Wind speed, Human activity

Citation: Zhang S, Xu H, Lan J, Goldsmith Y, Torfstein A, Zhang G, Zhang J, Song Y, Zhou K, Tan L, Xu S, Xu X, Enzel Y. 2021. Dust storms in northern China during the last 500 years. Science China Earth Sciences, 64(5): 813–824, https://doi.org/10.1007/s11430-020-9730-2

1. Introduction

Extensive areas of sand and deserts are present in the arid/semi-arid zone of northern China, where the East Asian summer monsoon (EASM) is weak. Large amounts of dust particles blown by strong winds from these areas form frequent dust storms, which have a marked effect on the regional climate (Shao et al., 2011), economic activity (Middleton, 2017), and human health (Middleton and Sternberg, 2013). The dust can be transported over thousands of kilometres and affect global climate processes (Shao et al., 2011), atmospheric chemistry (Middleton, 2017), and biogeochemical cycling (Falkowski et al., 1998). For example, a study has shown that Asian dust can be transported more than one full circle around the globe in approximately 13 days, which could influence the global radiation budget and marine ecosystems (Uno et al., 2009).

It is important to master the history and mechanisms of dust storms and predict their future occurrence. Observations can accurately monitor dust-storm activity at high temporal and spatial resolutions, up to daily and/or monthly scales. However, before the 1950s the observational data is scarce in northern China. In contrast, historical documents and geological archives can be used to determine the dust storm

* Corresponding author (email: xuhai@tju.edu.cn)

history on longer time scales. For example, Zhang (1984) extracted 1156 records from historical literatures relevant to dust falls for the last 1700 years. However, records of dust storm activity in historical documents are generally descriptive, and the storm intensity is difficult to quantify. Geological archives, such as lake sediments and ice cores, can provide histories of dust storms over longer time scales (Yang et al., 2006; Chen et al., 2013; Qiang et al., 2014; He et al., 2015; Zhang et al., 2015; Liu et al., 2019; Chen F et al., 2020) and have therefore been widely used to study dust storm history (He et al., 2015; Chen F et al., 2020; Chen S et al., 2020; Zhang et al., 2020). In particular, the sedimentary grain sizes of closed lakes have been shown to be sensitive to changes in dust storm activity and hence have been widely applied to trace historical dust storm occurrences. For example, Huang et al. (2011) recovered a 2000-yr history of dust storm activity in western central Asia, using both the grain-size fraction ratio between 6–32 μm and 2–6 μm, and Ti contents of Aral Sea sediments. Chen et al. (2013) reconstructed a 2000-yr-long dust storm history for the northern Tibetan Plateau, based on the coarse fraction (56–282.5μm) retrieved from Lake Sugan. Using grain-size analysis of Lake Xiarinur sediments, Xu et al. (2018) established a Holocene record of aeolian activity in northern China and proposed a decoupling between long-distance Asian dust export and climate aridity. A high-resolution Holocene record of aeolian activity was also reconstructed by Qiang et al. (2014) for Lake Genggahai, northeastern Tibetan Plateau, by using the sand fraction (>63 μm) as an indicator. However, most previous studies of historical dust storms have focused on the arid Tibetan Plateau and northwest China, where dust sources are widespread, and the history of dust storms in northern China remains less clear.

The mechanisms that control dust storms remain contentious. Precipitation has been assumed to be an important control on dust storm occurrence by affecting soil moisture and vegetation (Liu et al., 2004). However, Qian et al. (2002) argued that there was a significant correlation between dust storms and temperature, rather than precipitation, in eastern China. Whether high or low temperatures can enhance dust storm activity is still a matter of debate (Chen et al., 2013; Liu et al., 2015; He et al., 2015). In addition, it is still not clear whether human activity or natural factors are the major factors controlling the frequency, magnitude, and extent of dust storms. For example, Neff et al. (2008) studied changes in dust activity during the past 5000 yr in the western United States and ascribed the dramatically increased dust deposition in the early twentieth century to human activity. Recently, Chen F et al. (2020) studied the dust storm history at Lake Gonghai, northern China, and suggested that human activity may have surpassed natural factors and become the dominant factor in dust storms from at least 2000 years ago (Chen F et al., 2020); whereas authors also contend that the relationships between dust storms, climatic factors, and human activities differ in different regions (Chen S et al., 2020). Additional reliable long-term, high-resolution dust storm records are necessary to resolve these uncertainties.

Lake Daihai is a large closed-basin lake located in the EASM frontier zone in northern China. The lake is located near several deserts and therefore has a high potential of capturing past dust storm activity in northern China. In this study, we obtained a high-resolution record of the dust storm history of the last 500 years from a sediment core collected in this lake, and discussed the potential dust storm controlling mechanisms, including natural climate forcing and anthropogenic impacts.

2. Site setting

Lake Daihai (40°29′07″–40°37′06″N, 112°33′31″–112°46′40″E) is located on the northern fringe of the Chinese Loess Plateau. Several deserts are present in the surrounding area: the Badain Jaran Desert, the Tengger Desert, the Kubuqi Desert, and the Mu Us sandy land (Figure 1a), which are widely considered to be the dust sources for northern China. The surface area of the lake was ~133 km^2 (Wang and Dou, 1998) and has shrunk markedly during the past two decades. The catchment area of the lake is ~2290 km^2 (Wang and Dou, 1998). Mountains and hills are distributed in north, south, and east of the lake basin, and plains extend from the western shore. Five rivers enter the lake: The Muhua and Gongba rivers from the east and west, respectively, and three small intermittent streams from the south (Figure 1b; Xiao et al., 2013).

Strong winds occur in spring, influenced by both the Siberian High and the westerlies (Figure 1 and Supplementary Figure S1, http://link.springer.com). In summer, warm, moist air from low-latitude ocean regions can reach the lake area and bring precipitation. The mean annual temperature in the lake area is 5°C, with mean July and January temperatures of 20.5 and −13.1°C, respectively (Wang and Dou, 1998). The freezing interval is from December to March. Mean annual precipitation and evaporation are 423 and 1162 mm, respectively (Xiao et al., 2004, 2013). Modern vegetation in the basin varies from forest-shrub grassland to semi-arid grassland (Compilatory Commission of Annals of Liangcheng County, 1993).

Observational data from five meteorological stations around Lake Daihai (Datong, United Banner of Darhan and Maoming'an, Jining, Hohhot, and Taiyuan; Supplementary Figures S2 and S3 and Table S1) indicate that dust storms occur mainly from March to May, with the highest frequency in April and the lowest in August (Figure 1c). There is a significant positive correlation between wind speed and dust storm frequency (Figure 1c; r=0.89, p<0.01).

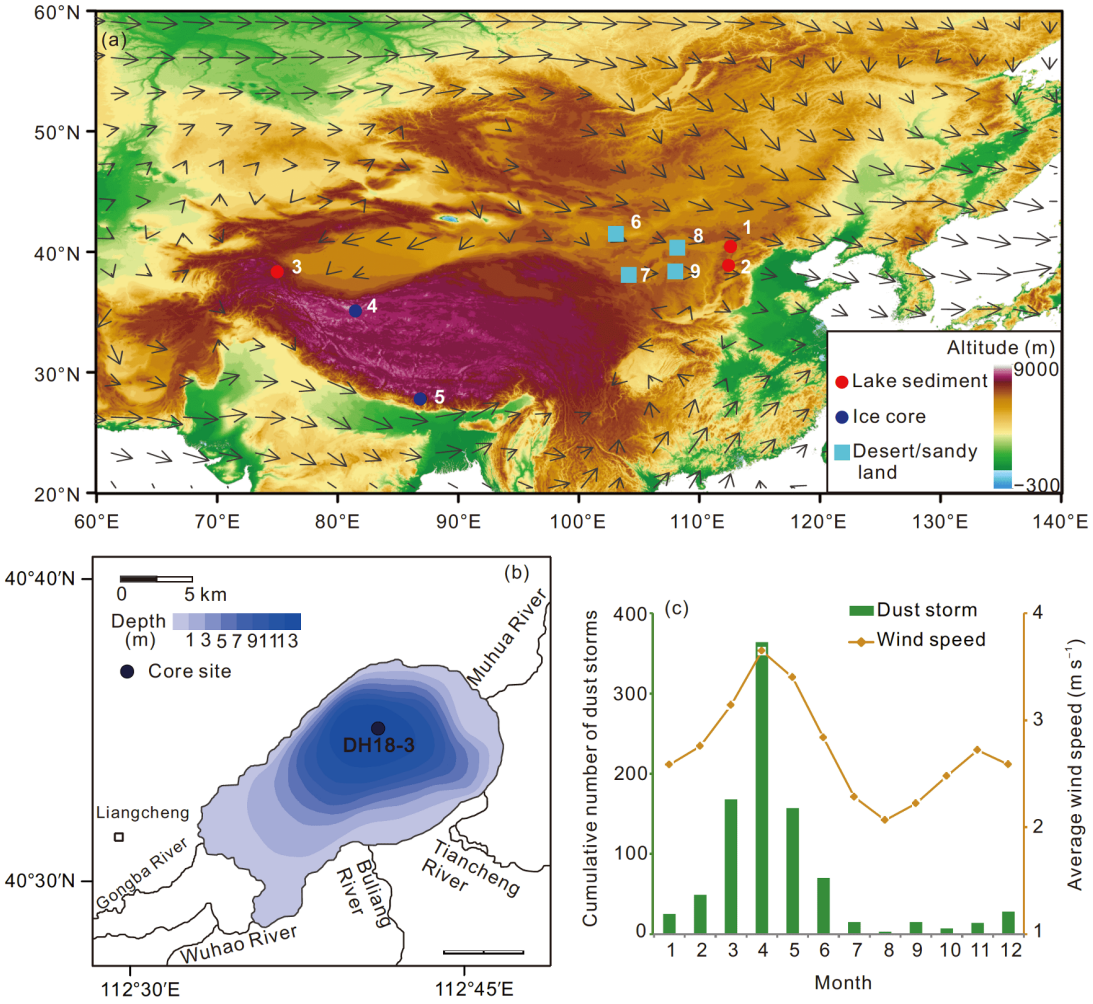

Figure 1 (a) Locations of Lake Daihai and other sites with dust storm records or deserts mentioned in this study. 1, Lake Daihai; 2, Lake Gonghai; 3, Lake Karakul; 4, Guliya ice core; 5, East Rongbuk ice core; 6, Badain Jaran Desert; 7, Tengger Desert; 8, Kubuqi Desert; 9, Mu Us sandy land. Arrows in panel (a) show the average spring wind fields at 850 hPa for ERA-Interim reanalysis data for AD 1979–2008 (Dee et al., 2011). (b) Lake Daihai and the core site. The lake isobaths are redrawn from Xiao et al. (2004). (c) Monthly distributions of cumulative dust-storm counts for AD 1954–2007 and the average wind speed at five meteorological stations (Datong, United Banner of Darhan and Maoming'an, Jining, Hohhot, and Taiyuan; Supplementary Figure S1 and Table S1, http://link.springer.com).

3. Material and methods

3.1 Sampling

In August 2018, a sediment core (40°35′06″N, 112°40′54″E; DH18-3, elevation: 1205 m a.s.l., water depth 6.9 m, core length ~1.87 m; 100% sediment recovery) was obtained from the deep-water area of Lake Daihai using a gravity corer (Figure 1b). The water-sediment interface is clear, suggesting that no strong disturbance occurred during the coring process. The sediment at 0–35.0 cm is black, at 35.0–169.5 cm is grey, and at 169.5–186.5 cm is blackish in colour. A total of 237 sediment samples were obtained from the core, at 0.5 cm intervals for the upper 50 cm and 1 cm intervals for the remainder (51–187 cm).

3.2 Chronology

The ^{137}Cs and ^{210}Pb activities of the freeze-dried sediment samples of core DH18-3 were measured using an Ortec Germanium (HPGe) well detector (GWL-250-15). Three pieces of plant debris and one plant seed (Figure 2) were picked from the core and were dated by radiocarbon dating at the University of California, Irvine, USA.

3.3 Grain-size analyses

The grain size of the sediment samples was analysed using a Malvern Mastersizer 2000 laser grain-size analyser. Approximately 1 g of freeze-dried sample was treated with 10% H_2O_2 to remove organic material, then treated with 10% HCl to remove carbonates, dispersed with 0.05 mol L^{-1} $(NaPO_3)_6$

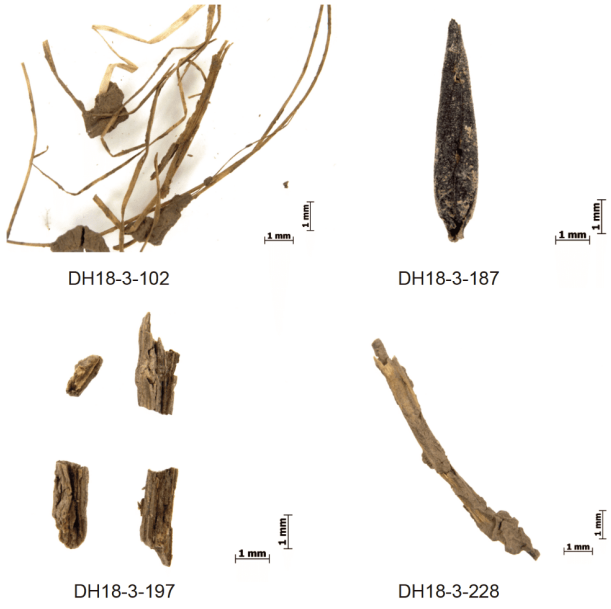

Figure 2 Samples selected for radiocarbon analyses from core DH18-3.

using an ultrasonic vibrator for 10 min, and transferred to the laser grain-size analyser.

4. Results

4.1 Age model

The ^{137}Cs activity profile of core DH18-3 is similar to the classic global atmospheric ^{137}Cs fallout pattern (Figure 3a; Bergan, 2002). Although ^{137}Cs diffusion may influence the amplitude and shape of the ^{137}Cs peak, the central position of the ^{137}Cs peak does not move (Xu H et al., 2010; Lan et al., 2020); consequently, the peaks can be used as reliable time-markers. Global multi-national above-ground nuclear weapon tests began in the early 1950s, and atmospheric ^{137}Cs fallout can be detected in lake sediments from approximately AD 1952 (Zhou et al., 2020). Therefore, the first ^{137}Cs time-marker (AD 1952) was assigned to the point (DH18-3-113, depth 63.0 cm) where ^{137}Cs activity began to increase (Figure 3a). Based on this time-marker, we calculated a mass accumulation rate of 0.48 g cm^{-2} yr^{-1}. The highest ^{137}Cs peak appeared at 49.5 cm (DH18-3-99), corresponding to the global atmospheric ^{137}Cs fallout peak at ~AD 1964 (Figure 3a; Xu H et al., 2010). The mass accumulation rate calculated from this time-marker is 0.46 g cm^{-2} yr^{-1}. The similar sedimentation rates calculated from these two independent ^{137}Cs time-markers suggest that the modern sedimentation rate in the deep central area of Lake Daihai has been relatively constant (at least after ~AD 1952). An age model of the upper 63 cm of the core was established by linear interpolation based on the ^{137}Cs time-markers (Figure 3c). The excess ^{210}Pb (^{210}Pb$_{ex}$) activity shows a classic pattern (Figure 3b). A constant rate of supply (CRS) ^{210}Pb$_{ex}$ age model (Appleby and Oldfield, 1978) was applied (Figure 3c), and the result is broadly consistent with the ^{137}Cs age model (Figure 3c).

The results of AMS ^{14}C dating are listed in Table 1. Sample DH18-3-102 is modern plant debris, as inferred from the ^{14}C value (108.91 pMC), which is higher than the value of 100 pMC at AD 1950. The corresponding age of this sample could be ~AD 1958 or ~AD 2000 by comparison with the modern atmospheric ^{14}C concentration curve (Figure 4a; http://calib.org/CALIBomb/), similar to the approach of Ely et al. (1992). Because sample DH18-3-102 is located between the two ^{137}Cs time-markers (DH18-3-113, AD 1952, and DH18-3-99, AD 1964), the age of sample DH18-3-102 is constrained to ~AD 1958 (Figure 4a). A combined age model of core DH18-3 (Figure 4b) was obtained by linear interpolation between the two ^{137}Cs time-markers and

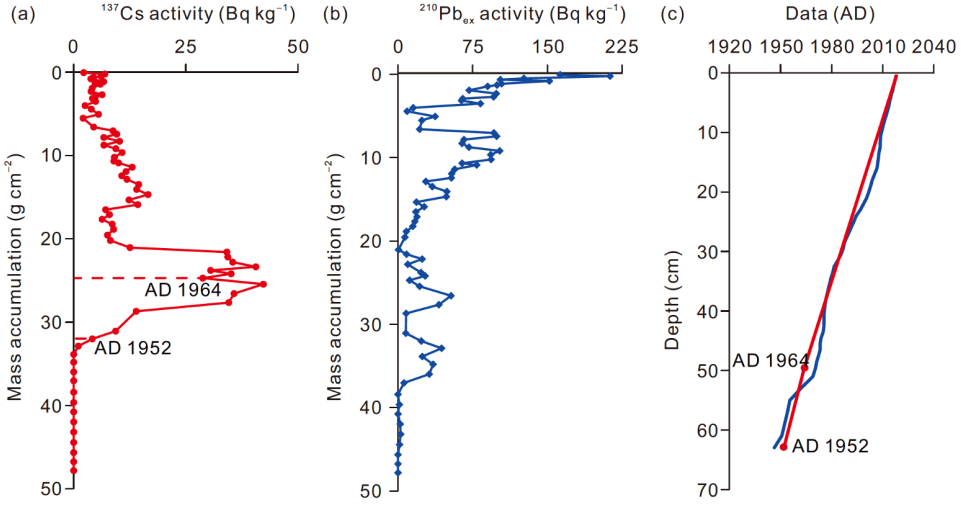

Figure 3 (a) ^{137}Cs activity, (b) ^{210}Pb$_{ex}$ activity, (c) ^{137}Cs age model (red curve) and ^{210}Pb$_{ex}$ CRS age model (blue curve; see text) for the upper 63 cm of core DH18-3. Note that the *y*-axes show mass accumulation in panels (a) and (b), but depth in panel (c).

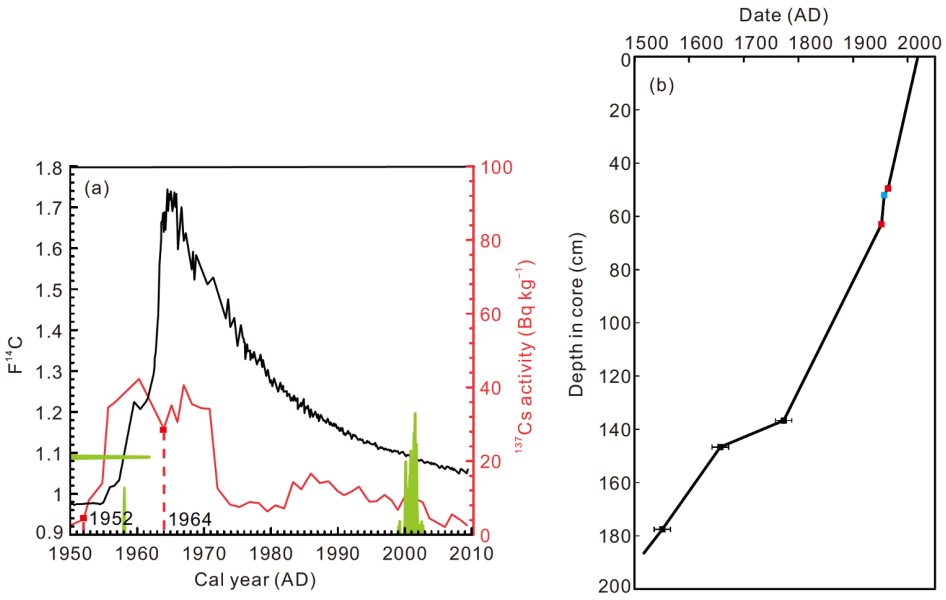

Figure 4 (a) Fraction of ^{14}C ($F^{14}C$) of sample DH18-3-102 (green curve), atmospheric ^{14}C concentration (black curve; http://calib.org/CALIBomb/), and ^{137}Cs activity (red curve; this study). (b) Age model of core DH18-3 established by linear interpolation between the two ^{137}Cs time-markers (AD 1952 and AD 1964, red points) and the four AMS ^{14}C ages (including the uncertainties, see details in Table 1). Black and blue points denote AMS ^{14}C ages older and younger than AD 1950, respectively (see text and Table 1 for details).

Table 1 AMS ^{14}C ages of samples from core DH18-3

Laboratory number	Sample number	Depth (cm)	Dating material	AMS ^{14}C age (yr BP)	Error (yr)	Calibrated median ^{14}C age (2σ) (cal yr BP) [a)]
UCIT38691	DH18-3-102	52	Plant debris	Modern		
UCIT38693	DH18-3-187	137	Plant seed	145	15	177
UCIT38694	DH18-3-197	147	Plant debris	240	15	293
UCIT38695	DH18-3-228	178	Plant debris	295	15	399

a) Calibrated by CALIB7.0.4 (Stuiver et al., 2017)

the four ^{14}C ages (Table 1), covering the last ~500 years from ~AD 1517 to 2018 (Figure 4b). The average temporal resolution for samples of the upper 50 cm is ~0.56 yr sample^{-1} (sectioned at 0.5 cm intervals), whereas the resolution for the lower section (51–187 cm; sectioned at 1 cm intervals) is ~3.25 yr sample^{-1}.

4.2 Grain size

The grain-size frequency distributions of most samples from core DH18-3 are unimodal, with only a few samples exhibiting a bimodal distribution (Figure 5). We divided the sediments into three fractions: clay (<4 μm), silt (4–63 μm), and sand (>63 μm), which account for ~13–45 vol.%, 54–87 vol.%, and 0–6 vol.%, respectively. The mean grain size varies from 6.0 to 14.8 μm (Figure 5a). The silt and clay fractions are highly negatively correlated with each other (r^2=0.98, p<0.001), whereas the sand fraction is not correlated with either the clay or the silt fraction (r^2=0.004, p<0.31, and r^2=0.04, p<0.002, respectively). End-member analysis of sedimentary grain size was also conducted, based on which the sediments could be statistically divided into three main components (see details in Supplementary Figures S4 and S5 and Tables S2 and S3). End member (EM) 1 and EM 3 are similar and reflect the clay and silt fractions, respectively. EM 2 reflects the sand fraction (Supplementary Figure S5). Evidence from a long core sampled previously in this lake (Peng et al., 2005) indicates that the absence of a correlation between sand and either clay or silt holds throughout the Holocene, suggesting that the sand fraction was controlled by a different process from that of the silt and clay fractions.

5. Discussion

5.1 Indicators of dust storms and comparisons with meteorological records

Sediments enter lakes by fluvial and aeolian processes. Using downcore grain-size data to distinguish between these two processes is complicated and requires a detailed site-specific understanding of the processes affecting sediment

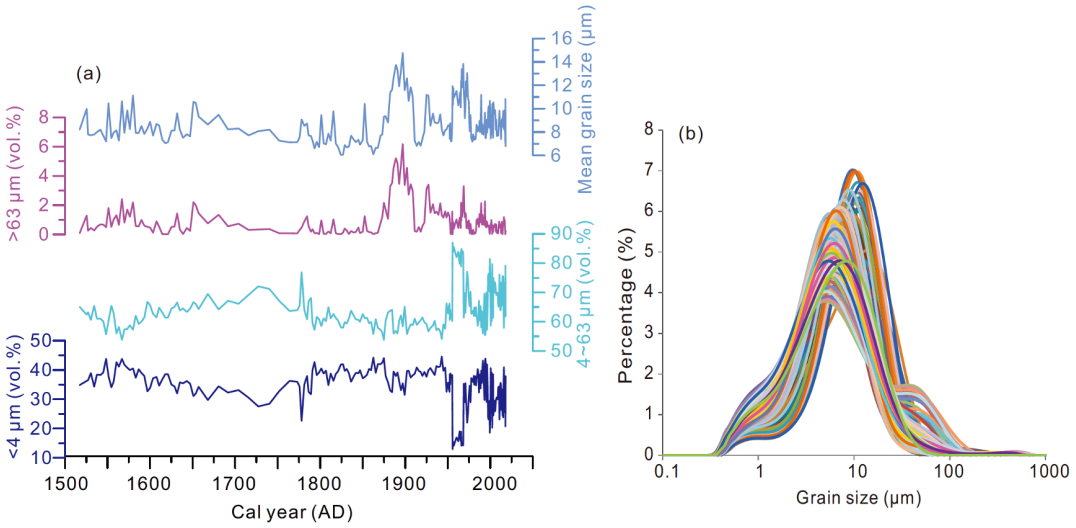

Figure 5 (a) Grain-size fractions and (b) grain-size frequency distributions of all sediment samples of core DH18-3.

influx into the lake. Here, we first characterise the modern sediment influx into the lake and then use this understanding of modern processes to reconstruct strong dust events over the past 500 years.

During the past 50 years, the silt and clay fractions in Lake Daihai changed markedly (Figure 5). To evaluate whether this change is a function of climatological parameters or lake levels, we compared the different grain-size fractions with rainfall and wind-speed data from Jining station, located 60 km northeast of Lake Daihai, and with modern lake-level changes (Supplementary Figure S6). The lake level dropped by ~10 m over the past 50 years (Supplementary Figure S6). This drop is inconsistent with the climatology and is most likely the result of enhanced human activity, like river water interception. If the sand fraction in Lake Daihai were brought by riverine runoff, then the recent decrease in lake level should have resulted in an increase in the abundance of coarse particles at the core site because the distance from the river mouth to the core site has been markedly shortened, opposite to the observed decreasing trend in the coarse fraction (Figure 6e). However, the finer fraction (4–63 μm) may be transported to the centre of the lake by means of suspension and saltation (Xiao et al., 2013). When the lake level drops, this component is likely to increase. The sharp increases in the 4–63 μm component after ~AD 1950 (Figure 5a) support such an inference. An alternative option is changes in wind speed, which can result in the transportation of different grain-size fractions to the lake. However, as the wind speed has dropped by ~50% over the past 50 years (see Supplementary Figure S6), the expected response would be a decrease in the silt fraction and an increase in the clay fraction, which does not agree with the observations. Therefore, we propose that the clay and silt fractions are related to the lake size and distance from the shore. The sand fraction is completely decoupled from the finer fractions and is therefore unlikely to have been derived from changes in runoff and lake size, making wind transport the most probable option for sand delivery.

Xiao et al. (2013) conducted a detailed study of the modern distribution of grain size in Lake Daihai and demonstrated that the sand fraction (C4 and C5 in that study) decreases as a function of distance from the shore. At distances greater than 1.5 km from the shore, almost no sand fraction is present in the modern core tops. In the present study, core DH18-3 was retrieved from the deepest part of the lake, which is ~2.4 km from the closest river mouth of a small intermittent river on the northern side of the lake (Figure 1b). Thus, in the present day, the coarse fraction (>63 μm) does not reach the core site, and there is no reason to assume that sand could have reached the core site when the lake was larger (e.g., 50 years ago). Therefore, additional transport mechanisms must be invoked to explain the presence of the sand fraction in the centre of the lake. Xiao et al. (2013) also showed that the aeolian dust that reaches Lake Daihai during winter and spring, when the lake is frozen over, has a grain-size that is much larger (modal size 50 μm) than that found in the suspended component of the lake sediments in the centre of the lake (modal size 16–32 μm). This finding also indicates that the coarse fraction in the centre of the lake is aeolian in origin rather than transported by runoff.

We also compiled modern dust-storm data observed at nine meteorological stations around Lake Daihai (Datong, United Banner of Darhan and Maoming'an, Jining, Hohhot, Huade, Taiyuan, Xing County, Siziwang Banner, and Beijing; see details in Supplementary Figures S2 and S3 and Table S1). These records show broadly similar trends to the variations in the coarse fraction in core DH18-3 from Lake Daihai (Figure 6d–6f). For these reasons, we conclude that the sand component (>63 μm) in lake sediment cores collected from the centre of Lake Daihai could not have been transported by

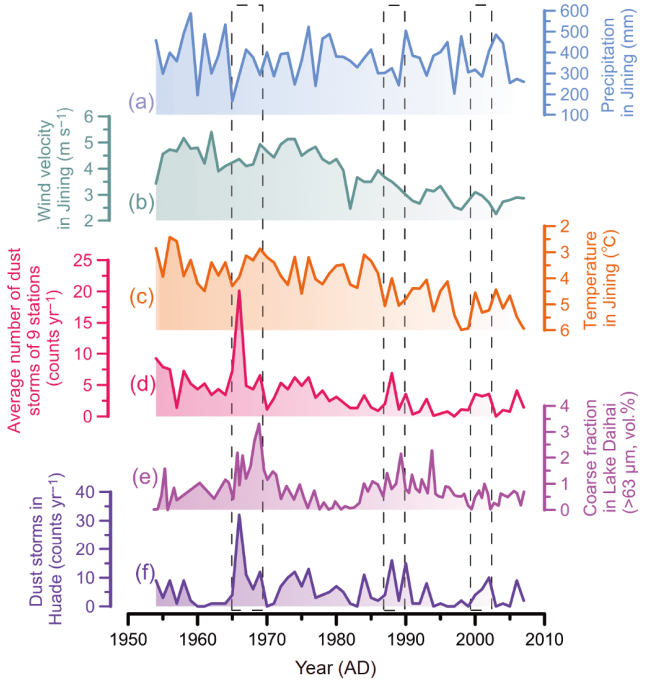

Figure 6 Comparison between the sedimentary coarse fraction (>63 μm; curve (e)) in core DH18-3 and other modern observed data for AD 1954–2007. (a) Mean annual precipitation in Jining. (b) Mean wind speed in Jining from March to May. (c) Mean annual temperature in Jining. Note that the temperature is plotted inversely. (d) Average dust-storm occurrences from nine meteorological stations (Datong, United Banner of Darhan and Maoming'an, Jining, Hohhot, Huade, Taiyuan, Xing County, Siziwang Banner, and Beijing; see details in Supplementary Figures S1 and S2 and Table S1). (f) Dust-storm frequency in Huade. The dashed vertical columns denote three modern intervals with frequent dust storms, broadly around AD 1965, 1988, and 2002.

riverine/surface runoff, and was most likely transported by strong winds, and can thus be used to indicate dust storms.

5.2 Reconstruction of dust-storm history for northern China

Dust storms in northern China, inferred from changes in the sand fraction (>63 μm) in core DH18-3, were strengthened during three intervals: AD 1520–1580, AD 1610–1720, and AD 1870–2000 (Figure 7e). The amplitudes during AD 1520–1580 and AD 1610–1720 were lower than those during AD 1870–2000. However, although dust-storm activity has on average intensified in the recent past (AD 1870–2000), there is a clear decreasing trend within this interval. This decreasing trend can also be detected in both observational data and other geological records (Figure 7; Zhang et al., 2020). An exception is the recent record at Lake Gonghai, where dust storms seem to have continued to increase during the past century (Chen F et al., 2020); however, Lake Gonghai is a relatively small lake, and intensive human activities, such as forest cutting and road construction, have occurred in this lake basin during recent decades. Excluding the grain-size data for Lake Gonghai after the 1970s, a broadly decreasing trend in dust storms can still be observed (Figure 7).

The dust-storm activities extracted from lake sediments are broadly synchronous with those recorded in historical documents (Figure 7a, 7b). However, there are clear differences in the dust-storm magnitudes inferred from grain size and those extracted from historical literature (Figure 7). We hypothesise that the historical records may be more accurate in recording the timing and frequency of dust storms, whereas the estimated intensities of these storms may be less reliable owing to the difficulty in quantifying the historical records. There are also some slight inconsistencies in the timings of the proxy-based dust storms inferred from the different curves illustrated in Figure 7, which may be partly ascribed to the processes responsible for recording the dust storms in different archives. For example, lake sediments record dust storms by capturing the local coarse particles, whereas glaciers capture dust storms by enclosing fine particles from remote sources. The chronologies may also contain some uncertainties because of differences in dating of different archives. In addition, the records presented in Figure 7 represent dust storms in different regions, and it is reasonable to expect some spatial differences. The dust storms captured in Lake Daihai over the past 100 years show a high degree of resemblance to those in Lake Karakul (Zhang et al., 2020), the East Rongbuk ice core (Xu J et al., 2010), the Guliya ice core (Thompson et al., 1995), and Lake Gonghai (Chen F et al., 2020) (Figure 7). These similar, broad-scale patterns further support our interpretation of the coarse fraction in Lake Daihai as aeolian indicators and not localised riverine runoff intensity.

5.3 Possible forcing mechanisms of dust storms

The occurrence of dust storms is controlled by the combined effect of various factors, including temperature, precipitation, wind speed, and human activity. Dust sources and strong winds are the major factors influencing dust storm outbreaks, and both are affected by climate, environment, and human activity. In general, temperature has an important influence on wind speed, precipitation is important for the regional vegetation biomass, and human activity can influence both vegetation cover and dust-particle supply. As climatic patterns, vegetation cover, regional geomorphology, and anthropogenic impacts differ between regions, the relationships between dust storms, climatic parameters, and human activities should also vary geographically (e.g., Chen S et al., 2020).

5.3.1 Climatic forcing

(i) Temperature. Temperature trends have been broadly synchronous over different regions in China during the past several centuries (Wang et al., 2007; Ge et al., 2011). In the

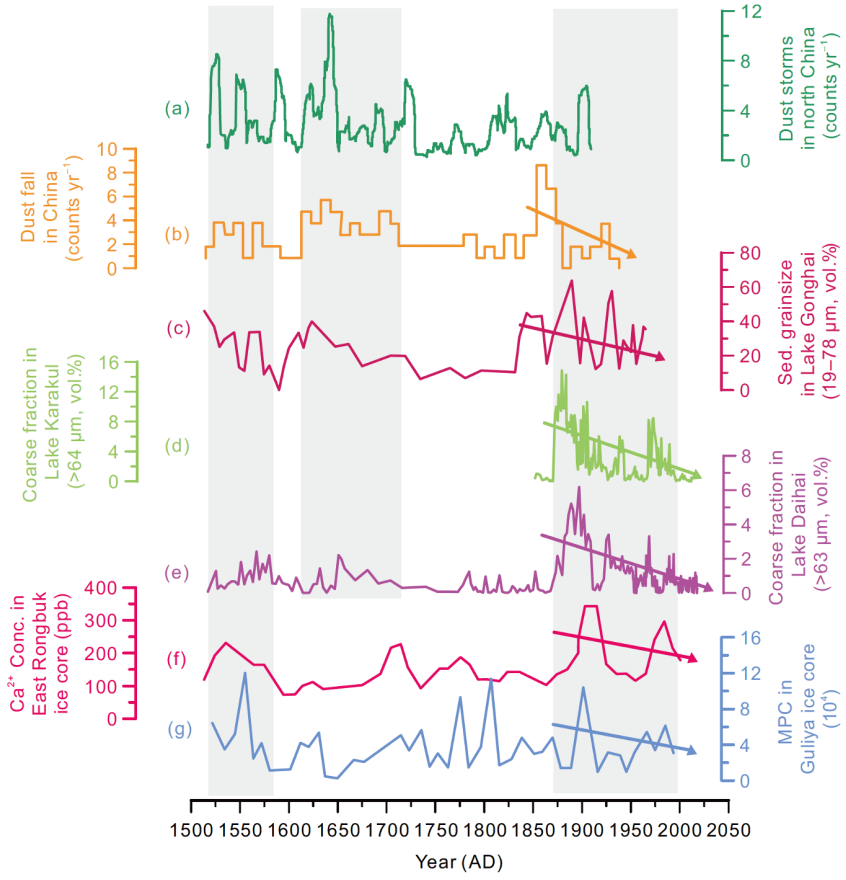

Figure 7 Dust storms in Lake Daihai and in other records. (a) Ten-year moving average of dust-storm frequency in northern China recorded in historical literature (Deng and Jiang, 2006). (b) Dust-fall frequency in China recorded in historical literature (Zhang, 1984). (c) Lake Gonghai 19–78 μm component (Chen F et al., 2020). Note that these records are not plotted for the period after the 1970s because intensive local forest cutting and road construction around this lake during recent decades may have masked the real dust-storm signals (see text). (d) Lake Karakul >64 μm component (Zhang et al., 2020) . (e) Lake Daihai >63 μm component (this study). (f) Ten-year moving average of the Ca^{2+} concentration of the East Rongbuk ice core (Xu J et al., 2010). (g) Ten-year moving average of microparticle concentrations (MPC; ≥2 μm) per millilitre sample of the Guliya ice core (Thompson et al., 1995). The shaded grey bars indicate intense dust-storm intervals.

present study, we use the winter half-year temperature anomaly in eastern China (Ge et al., 2011) to represent the temperature conditions in northern China. Dust storms generally occurred in cold intervals during the past 500 years (Figure 8d–8f), and modern dust storm occurrence also shows a negative correlation with temperature (Figure 6c–6f). Dust storm records from other geological archives also indicate greater dust generation during cold periods. For example, the dust deposition rate has been estimated at 25 times higher in glacial than interglacial periods, based on records obtained from Antarctica ice cores (EPICA Dome C; Lambert et al., 2008). In marine sedimentary records, the dust deposition rate is three to five times higher in glacial periods than interglacial ones (Rea, 1994). Huang et al. (2011) showed that dust storms recorded in Aral Sea sediments are highly correlated with temperature and the Siberian High, with enhanced aeolian activities corresponding to low temperature and strengthened Siberian High, and vice versa. Qiang et al. (2014) found that episodically enhanced aeolian activities were correlated with cold events, as inferred from the sedimentary sand fraction at Lake Genggahai, northeastern Tibetan Plateau. Liu et al. (2019) presented a ~40 kyr record of dust activity at Lop Nur palaeo-lake on the eastern margin of the Tarim Basin and they also suggested that the cold events could be the dominant controlling factors of dust storm outbreaks. Dust storms recorded in historical records for AD 1464–1913 show a significant negative correlation with spring and winter temperature variations (Deng and Jiang, 2006). Observational data from 338 stations in China from AD 1950 to 1998 also show a significant negative correlation between dusty periods and temperature (r=−0.68) (Qian et al., 2002).

(ii) Wind speed. High wind speed has been demonstrated to be the primary factor controlling dust storm outbreaks (Lee and Sohn, 2009; Roe, 2009; Lee and Kim, 2012). The minimum wind speed triggering dust storms varies with different land surface conditions, and a speed of 6.5 m s^{-1} has been widely used as the critical wind speed in numerical simulations (Tegen and Fung, 1994; Roe, 2009). In northern China, variations in both the Siberian High and the intensity

of westerlies can influence wind speed and thereby dust storm occurrences. Roe (2009) argued that in China, strong winds occur during spring when tropical heat propagates northward, breaking down the Siberian High and producing atmospheric instabilities, high wind speeds, and large dust storms. The dust storm record from Lake Sugan has shown that frequent and intensive dust storms are associated with strengthening Siberian High (Chen et al., 2013). Xu et al. (2018) proposed that the Siberian High plays an important role in long-distance transportation of Asian dust particles. Modern dust storms occur mainly during periods with high wind speeds (Figure 6b, 6d–6f), and historical dust storm activity is also broadly synchronous with the years of frequent high-speed winds disasters/hazards (Figure 8a).

The Westerlies are also intensified during colder spells and may contribute to higher dust storm intensity and frequency. Meteorological records show that in years with intense dust storms, westerlies in northern China tend to move southwards and intensify (Zhong and Li, 2005). Dust storm trends are similar in cores from Lake Daihai and Lake Gonghai, and Lake Karakul, the Guliya ice core, and the East Rongbuk ice core (see locations in Figure 1), supporting the hypothesis that westerly winds are a common driving force. The East Rongbuk ice core is located at a lower latitude and is likely to have been influenced by the southern branch of westerly winds.

(iii) Precipitation. Particles in dust storms are derived from both distant and local sources. In general, the local particle supply is closely related to surface conditions, such as soil moisture content and vegetation cover. Precipitation is an important factor influencing local soil moisture content and vegetation cover; however, there is no significant correlation between dust storm activity and precipitation in the study area (Figures 6 and 8). According to meteorological data, the aridity index (aridity index=precipitation/potential evaporation) of most regions in northern China is below 0.5 (Yang et al., 2003). In the Lake Daihai area, mean annual evaporation is approximately three times higher than mean annual precipitation (Xiao et al., 2004), meaning that changes in precipitation may have less effect on local humidity relative to changes in evaporation. Furthermore, data on pollen assemblages have shown that Chenopodiaceae and *Artemisia* have prevailed in the Lake Daihai area over the past 600 years (Zhang, 2009). Although changes in precipitation would influence the local steppe biomass, the vegetation cover may change less markedly and may play only a limited role in modulating dust storm activity in this catchment. A previous study has suggested that dust storms are more frequent when annual precipitation is between 100–200 mm, but the correlation is weak for annual precipitation greater than 200 mm (Goudie, 1983). Similarly, a significant negative correlation has been established between precipitation and dusty weather in arid Xinjiang Province, northwestern China, but not in eastern China (Qian et al., 2002). Overall, precipitation in the study area is neither high enough to suppress dust storms nor low enough to activate them. Therefore, we conclude that precipitation has a relatively weak impact on the occurrence of short-term dust storms in the study area.

5.3.2 Potential dust sources and the influence of human activity

Dust storms in northern China may originate from both distant and local sources. Zhang and Gao (2007) estimated that approximately 70% of the dust storms that affected China during AD 2000–2002 came from Mongolia (Zhang and Gao, 2007). Observational data have suggested that arid regions with high levels of wind erosion in northern China, including the Taklimakan Desert, Hexi Corridor, Dunhuang region, Mu Us sandy land, Hunshadake sandy land, and Horqin sandy land, are potential sources of dust (Wang et al., 2015). Water vapour back trajectories at Lake Daihai (Supplementary Figure S1) also suggest that the dust is likely to have come from these areas. Local particles may also account for a considerable proportion of dust. For example, Zhao et al. (2007) analysed a dust storm event in Beijing and found that local particles were an important part of the sediment. Enzel et al. (2010) have also pointed out that fine sands (i.e., >63 μm) are very local in origin, similar to the sandy loess. Therefore, it is most likely that the sedimentary coarse fraction (>63 μm) deposited in the central deep area of Lake Daihai is derived mainly from local sources.

As mentioned above, during the recent warming epoch, average dust storm activity has been high, which appears to be inconsistent with the above-mentioned negative relationship between dust storm events and temperature. This inconsistency is likely due to the increased dust-particle supply during the Anthropocene. The population increased markedly after the nineteenth century, and large-scale migration into northern China occurred during the late Qing dynasty, especially land reclamation in the Tianshan piedmont, Hexi Corridor, Ordos Plateau, and Horqin region, etc. (Hu et al., 1999). Abandoned farmlands, deteriorated grasslands, and reactivated sand dunes may have accelerated desertification around the study area, providing large amounts of dust particles for dust storms. Approximately 17 intense dust storms occurred in the nineteenth century, as inferred from historical records (Hu et al., 1999), synchronous with the sharp increase in dust storm activity during AD 1870–1920 as shown in Figures 7 and 8. Analysis shows that desertified lands caused by over-cultivation, overgrazing, and over-forest-cutting constitute 25.4%, 28.3%, and 31.8% of the total area of desertified lands in northern China, respectively (Wang, 2004). The annual rate of desertification was 1560 km^2 from the late 1950s to the mid-1970s, increasing to 2100 km^2 during AD 1976–1988, and reaching

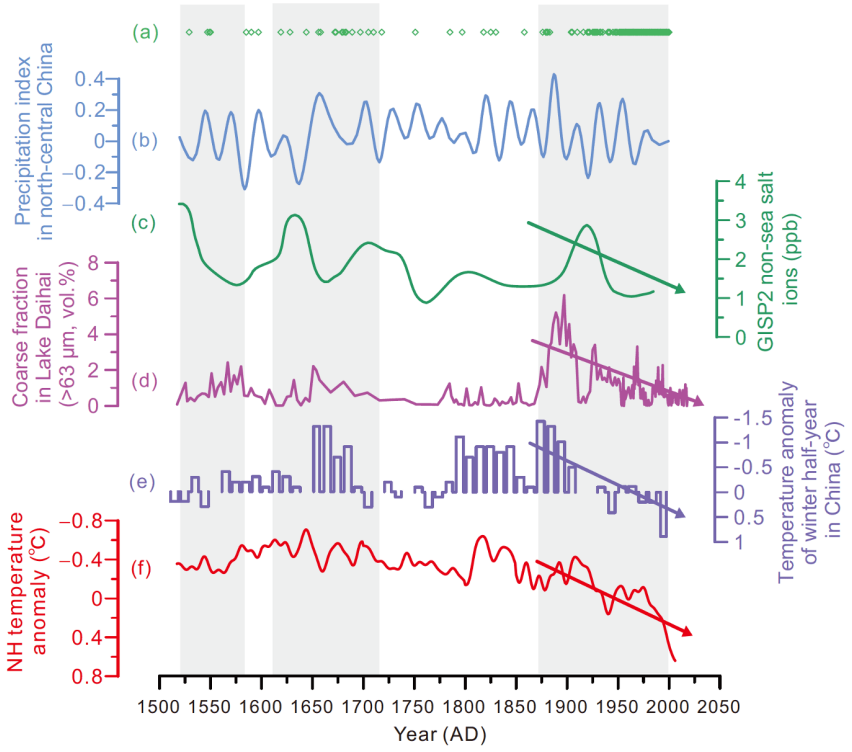

Figure 8 Dust-storm activity and potential influencing factors in northern China. (a) Strong winds leading to disasters/hazards in Inner Mongolia (Shen, 2008). (b) Precipitation index for north-central China (Yi et al., 2012). (c) GISP2 record of non-sea salt ions ($nssK^+$), indicating variations in the Siberian High (Mayewski and Maasch, 2006). (d) Lake Daihai >63 μm sediment component (this study). (e) Temperature anomaly of the winter half-year in eastern China (Ge et al., 2002). (f) Temperature anomaly in the Northern Hemisphere (NH) (Mann et al., 2009). Note that temperature anomalies are plotted inversely. The shaded grey bars indicate intervals of intense dust storms.

3600 km^2 during AD 1988–2000. The area of desertified land reached 38.57×10^4 km^2 in northern China in AD 2000 (Wang, 2004). Those extended desertified lands could have provided dust particles for northern China.

Although recent human activities could have increased the dust-particle supply, the timing of the dust storms is still approximately coeval with cold events (Zhang et al., 2020). In addition, dust storms exhibit a decreasing trend with the warming trend of the last century (Figures 6–8), which is consistent with the above-mentioned pattern that colder conditions lead to higher wind speeds and therefore greater dust-storm activity. Over the past 100 yr, the temperatures of China and the Northern Hemisphere have exhibited an overall increasing trend (Figure 8e, 8f). Recent global warming could have reduced the sea-land temperature difference and the temperature gradient in the winter half of the year, leading to weakening of the Siberian High and westerly winds (Grigholm et al., 2015) and, in turn, to the decreasing dust storm trend.

6. Conclusions

We constructed a high-resolution dust-storm history for northern China spanning the last 500 years based on the sand component (>63 μm) of a sediment core in Lake Daihai. There were three main dust-storm intervals: AD 1520–1580, AD 1610–1720, and AD 1870–2000. Dust storm activity systematically intensified but showed an obvious decreasing trend from AD 1870 to 2000. Changes in the intensities of the Siberian High and westerly winds, which are closely related to temperature variations, seem to have been the major factors controlling the occurrence of dust storms over northern China over the studied period. Recent global warming could have reduced the temperature gradient in the winter half-year, leading to a reduction in average wind speed and decreasing dust storm trend. Human activity has influenced the supply of dust particles and has therefore affected dust storm occurrence, especially during the past century. Given the continuing global warming, dust storm activity in northern China is expected to further weaken or remain at its present low level.

Acknowledgements *This work was supported by the National Natural Science Foundation of China (Grant No. U20A2078) and the Joint NSFC-ISF Research Program (NSFC Grant No. 41761144070; ISF Grant No. 2487/17).*

References

Appleby P G, Oldfield F. 1978. The calculation of lead-210 dates assuming

a constant rate of supply of unsupported ^{210}Pb to the sediment. Catena, 5: 1–8
Bergan T D. 2002. Radioactive fallout in Norway from atmospheric nuclear weapons tests. J Environ Radioact, 60: 189–208
Chen F, Chen S, Zhang X, Chen J, Wang X, Gowan E J, Qiang M, Dong G, Wang Z, Li Y, Xu Q, Xu Y, Smol J P, Liu J. 2020. Asian dust-storm activity dominated by Chinese dynasty changes since 2000 BP. Nat Commun, 11: 992
Chen F, Qiang M, Zhou A, Xiao S, Chen J, Sun D. 2013. A 2000-year dust storm record from Lake Sugan in the dust source area of arid China. J Geophys Res Atmos, 118: 2149–2160
Chen S, Liu J, Chen J, Chen F. 2020. Differences in the evolutionary pattern of dust storms over the past 2000 years between eastern and western China and the driving mechanisms. Sci China Earth Sci, 63: 1422–1424
Compilatory Commission of Annals of Liangcheng County. 1993. Annals of Liangcheng County (in Chinese). Hohhot: People's Press of Inner Mongolia. 100
Dee D P, Uppala S M, Simmons A J, Berrisford P, Poli P, Kobayashi S, Andrae U, Balmaseda M A, Balsamo G, Bauer P, Bechtold P, Beljaars A C M, van de Berg L, Bidlot J, Bormann N, Delsol C, Dragani R, Fuentes M, Geer A J, Haimberger L, Healy S B, Hersbach H, Hólm E V, Isaksen L, Kållberg P, Köhler M, Matricardi M, McNally A P, Monge-Sanz B M, Morcrette J J, Park B K, Peubey C, de Rosnay P, Tavolato C, Thépaut J N, Vitart F. 2011. The ERA-Interim reanalysis: Configuration and performance of the data assimilation system. Q J R Meteorol Soc, 137: 553–597
Deng H, Jiang W. 2006. Spatial and temporal characteristics of sandstorm activity in north China from 1464 to 1913 AD (in Chinese). Prog Nat Sci, 16: 86–93
Ely L L, Webb R H, Enzel Y. 1992. Accuracy of post-bomb ^{137}Cs and ^{14}C in dating fluvial deposits. Quat Res, 38: 196–204
Enzel Y, Amit R, Crouvi O, Porat N. 2010. Abrasion-derived sediments under intensified winds at the latest Pleistocene leading edge of the advancing Sinai-Negev erg. Quat Res, 74: 121–131
Falkowski P G, Barber R T, Smetacek V. 1998. Biogeochemical controls and feedbacks on ocean primary production. Science, 281: 200–206
Ge Q, Zheng J, Fang X, Man Z, Zhang X, Zhang P, Wang W-C. 2002. Temperature changes of winter-half-year in eastern China during the past 2000 years (in Chinese). Quat Sci, 22: 166–173
Ge Q S, Zhang X Z, Hao Z X, Zheng J Y. 2011. Rates of temperature change in China during the past 2000 years. Sci China Earth Sci, 54: 1627–1634
Goudie A S. 1983. Dust storms in space and time. Prog Phys Geography-Earth Environ, 7: 502–530
Grigholm B, Mayewski P A, Kang S, Zhang Y, Morgenstern U, Schwikowski M, Kaspari S, Aizen V, Aizen E, Takeuchi N, Maasch K A, Birkel S, Handley M, Sneed S. 2015. Twentieth century dust lows and the weakening of the westerly winds over the Tibetan Plateau. Geophys Res Lett, 42: 2434–2441
He Y, Zhao C, Song M, Liu W, Chen F, Zhang D, Liu Z. 2015. Onset of frequent dust storms in northern China at ~AD 1100. Sci Rep, 5: 17111
Hu J, Cui H, Tang Z. 1999. Temporal and spatial characteristics of sandstorm in China and the influences or human activities on its development trend (in Chinese). J Nat Resour, 8: 49–56
Huang X, Oberhänsli H, von Suchodoletz H, Sorrel P. 2011. Dust deposition in the Aral Sea: Implications for changes in atmospheric circulation in central Asia during the past 2000 years. Quat Sci Rev, 30: 3661–3674
Lambert F, Delmonte B, Petit J R, Bigler M, Kaufmann P R, Hutterli M A, Stocker T F, Ruth U, Steffensen J P, Maggi V. 2008. Dust-climate couplings over the past 800,000 years from the EPICA Dome C ice core. Nature, 452: 616–619
Lan J, Wang T, Chawchai S, Cheng P, Zhou K, Yu K, Yan D, Wang Y, Zang J, Liu Y, Tan L, Ai L, Xu H. 2020. Time marker of ^{137}Cs fallout maximum in lake sediments of Northwest China. Quat Sci Rev, 241: 106413
Lee E H, Sohn B J. 2009. Examining the impact of wind and surface vegetation on the Asian dust occurrence over three classified source regions. J Geophys Res, 114: D06205
Lee J J, Kim C H. 2012. Roles of surface wind, NDVI and snow cover in the recent changes in Asian dust storm occurrence frequency. Atmos Environ, 59: 366–375
Liu J, Wang R, Zhao Y, Yang Y. 2019. A 40,000-year record of aridity and dust activity at Lop Nur, Tarim Basin, northwestern China. Quat Sci Rev, 211: 208–221
Liu X, Yin Z Y, Zhang X, Yang X. 2004. Analyses of the spring dust storm frequency of northern China in relation to antecedent and concurrent wind, precipitation, vegetation, and soil moisture conditions. J Geophys Res, 109: D16210
Liu X, Yu Z, Dong H, Chen H F. 2015. A less or more dusty future in the Northern Qinghai-Tibetan Plateau? Sci Rep, 4: 6672
Mann M E, Zhang Z, Rutherford S, Bradley R S, Hughes M K, Shindell D, Ammann C, Faluvegi G, Ni F. 2009. Global signatures and dynamical origins of the Little Ice Age and medieval climate anomaly. Science, 326: 1256–1260
Mayewski P A, Maasch K A. 2006. Recent warming inconsistent with natural association between temperature and atmospheric circulation over the last 2000 years. Clim Past Discuss, 2: 327–355
Middleton N J. 2017. Desert dust hazards: A global review. Aeolian Res, 24: 53–63
Middleton N J, Sternberg T. 2013. Climate hazards in drylands: A review. Earth-Sci Rev, 126: 48–57
Neff J C, Ballantyne A P, Farmer G L, Mahowald N M, Conroy J L, Landry C C, Overpeck J T, Painter T H, Lawrence C R, Reynolds R L. 2008. Increasing eolian dust deposition in the western United States linked to human activity. Nat Geosci, 1: 189–195
Peng Y, Xiao J, Nakamura T, Liu B, Inouchi Y. 2005. Holocene East Asian monsoonal precipitation pattern revealed by grain-size distribution of core sediments of Daihai Lake in Inner Mongolia of north-central China. Earth Planet Sci Lett, 233: 467–479
Qian W, Quan L, Shi S. 2002. Variations of the dust storm in China and its climatic control. J Clim, 15: 1216–1229
Qiang M, Liu Y, Jin Y, Song L, Huang X, Chen F. 2014. Holocene record of eolian activity from Genggahai Lake, northeastern Qinghai-Tibetan Plateau, China. Geophys Res Lett, 41: 589–595
Rea D K. 1994. The paleoclimatic record provided by eolian deposition in the deep sea: The geologic history of wind. Rev Geophys, 32: 159–195
Roe G. 2009. On the interpretation of Chinese loess as a paleoclimate indicator. Quat Res, 71: 150–161
Shao Y, Wyrwoll K H, Chappell A, Huang J, Lin Z, McTainsh G H, Mikami M, Tanaka T Y, Wang X, Yoon S. 2011. Dust cycle: An emerging core theme in Earth system science. Aeolian Res, 2: 181–204
Shen J. 2008. Inner Mongolia Volume of China Meteorological Disaster (in Chinese). Beijing: Meteorological Publishing House. 138–165
Stuiver M, Reimer P J, Reimer R W. 2017. CALIB 7.0.4 [WWW program] at http://calib.org
Tegen I, Fung I. 1994. Modeling of mineral dust in the atmosphere: Sources, transport, and optical thickness. J Geophys Res, 99: 22897–22914
Thompson L G, Mosley-Thompson E, Davis M E, Lin P N, Dai J, Bolzan J F, Yao T. 1995. A 1000 year climate ice-core record from the Guliya ice cap, China: Its relationship to global climate variability. Ann Glaciol, 21: 175–181
Uno I, Eguchi K, Yumimoto K, Takemura T, Shimizu A, Uematsu M, Liu Z, Wang Z, Hara Y, Sugimoto N. 2009. Asian dust transported one full circuit around the globe. Nat Geosci, 2: 557–560
Wang H, Jia X, Li K, Li Y. 2015. Horizontal wind erosion flux and potential dust emission in arid and semiarid regions of China: A major source area for East Asia dust storms. Catena, 133: 373–384
Wang S, Dou H. 1998. Annals of Lakes in China (in Chinese). Beijing: Science Press. 325–327
Wang S, Wen X, Luo Y, Dong W, Zhao Z, Yang B. 2007. Temperature reconstructions in China over the last 1000 years (in Chinese). Chin Sci

Bull, 8: 958–964
Wang T. 2004. Progress in sandy desertification research of China. J Geogr Sci, 14: 387–400
Xiao J, Fan J, Zhou L, Zhai D, Wen R, Qin X. 2013. A model for linking grain-size component to lake level status of a modern clastic lake. J Asian Earth Sci, 69: 149–158
Xiao J, Xu Q, Nakamura T, Yang X, Liang W, Inouchi Y. 2004. Holocene vegetation variation in the Daihai Lake region of north-central China: A direct indication of the Asian monsoon climatic history. Quat Sci Rev, 23: 1669–1679
Xu B, Wang L, Gu Z, Hao Q, Wang H, Chu G, Jiang D, Liu Q, Qin X. 2018. Decoupling of climatic drying and Asian dust export during the Holocene. J Geophys Res Atmos, 123: 915–928
Xu H, Liu X Y, An Z S, Hou Z H, Dong J B, Liu B. 2010. Spatial pattern of modern sedimentation rate of Qinghai Lake and a preliminary estimate of the sediment flux. Chin Sci Bull, 55: 621–627
Xu J, Hou S, Qin D, Kaspari S, Mayewski P A, Petit J R, Delmonte B, Kang S, Ren J, Chappellaz J, Hong S. 2010. A 108.83-m ice-core record of atmospheric dust deposition at Mt. Qomolangma (Everest), central Himalaya. Quat Res, 73: 33–38
Yang J, Ding Y, Chen R, Liu L. 2003. Variations of precipitation and evaporation in north China in recent 40 years (in Chinese). J Arid Land Resour Environ, 17: 8–13
Yang M, Yao T, Wang H. 2006. Microparticle content records of the Dunde ice core and dust storms in northwestern China. J Asian Earth Sci, 27: 223–229
Yi L, Yu H, Ge J, Lai Z, Xu X, Qin L, Peng S. 2012. Reconstructions of annual summer precipitation and temperature in north-central China since 1470 AD based on drought/flood index and tree-ring records. Clim Change, 110: 469–498
Zhang D. 1984. Synoptic-climatic studies of dust fall in China since historic times. Sci China: Ser B, 825–836
Zhang J, Xu H, Lan J, Ai L, Sheng E, Yan D, Zhou K, Yu K, Song Y, Zhang S, Torfstein A. 2020. Weakening dust storm intensity in arid central Asia due to global warming over the past 160 years. Front Earth Sci, 8: 284
Zhang K, Gao H. 2007. The characteristics of Asian-dust storms during 2000–2002: From the source to the sea. Atmos Environ, 41: 9136–9145
Zhang L. 2009. Quantitative restoration of vegetation and climate change in Daihai basin in the past 600 years using sporopollen data. Master Dissertation (in Chinese). Shijiazhuang: Hebei Normal University
Zhang Y, Kang S, Zhang Q, Grigholm B, Kaspari S, You Q, Qin D, Mayewski P A, Cong Z, Huang J, Sillanpää M, Chen F. 2015. A 500-year atmospheric dust deposition retrieved from a Mt. Geladaindong ice core in the central Tibetan Plateau. Atmos Res, 166: 1–9
Zhao X, Zhuang G, Wang Z, Sun Y, Wang Y, Yuan H. 2007. Variation of sources and mixing mechanism of mineral dust with pollution aerosol—Revealed by the two peaks of a super dust storm in Beijing. Atmos Res, 84: 265–279
Zhong H, Li D. 2005. Relationship between sand dust storm in northern China in April and Westerly Circulation (in Chinese). Plateau Meteorol, 24: 104–111
Zhou K, Xu H, Lan J, Yan D, Sheng E, Yu K, Song Y, Zhang J, Fu P, Xu S. 2020. Variable late Holocene ^{14}C reservoir ages in Lake Bosten, Northwestern China. Front Earth Sci, 7: 328

(Responsible editor: Jule XIAO)